Cerebral Cortex, May 2016;26: 1866–1877

doi: 10.1093/cercor/bhu313
Advance Access Publication Date: 21 January 2015
Original Article

ORIGINAL ARTICLE

Triggering Different Brain States Using Asynchronous Serial Communication to the Rat Amygdala

Flávio Afonso Gonçalves Mourão, André Luiz Vieira Lockmann, Gabriel Perfeito Castro, Daniel de Castro Medeiros, Marina Pádua Reis, Grace Schenatto Pereira, André Ricardo Massensini, and Marcio Flávio Dutra Moraes

Núcleo de Neurociências (NNC), Departamento de Fisiologia e Biofísica, Instituto de Ciências Biológicas, Universidade Federal de Minas Gerais. Av. Antônio Carlos, Belo Horizonte, Minas Gerais, Brazil

Address correspondence to M.F.D. Moraes, NNC—Departamento de Fisiologia e Biofísica, Instituto de Ciências Biológicas, Universidade Federal de Minas Gerais. Av. Antonio Carlos, 6627, CEP 31270-901 Campus Pampulha, Belo Horizonte, Minas Gerais, Brazil. Email: mfdm@icb.ufmg.br

Abstract

Inputting information to the brain through direct electrical microstimulation must consider how underlying neural networks encode information. One unexplored possibility is that a single electrode delivering temporally coded stimuli, mimicking an asynchronous serial communication port to the brain, can trigger the emergence of different brain states. This work used a discriminative fear-conditioning paradigm in rodents in which 2 temporally coded microstimulation patterns were targeted at the amygdaloid complex. Each stimulus was a binary-coded "word" made up of 10 ms bins, with 1's representing a single pulse stimulus: A-1001111001 and B-1110000111. During 3 consecutive retention tests (i.e., day-word: 1-B; 2-A, and 3-B), only binary-coded words previously paired with a foot-electroshock elicited proper aversive behavior. To determine the neural substrates recruited by the different stimulation patterns, c-Fos expression was evaluated 90 min after the last retention test. Animals conditioned to word-B, after stimulation with word-B, demonstrated increased hypothalamic c-Fos staining. Animals conditioned to word-A, however, showed increased prefrontal c-Fos labeling. In addition, prefrontal-cortex and hypothalamic c-Fos staining for, respectively, word-B- and word-A-conditioned animals, was not different than that of an unpaired control group. Our results suggest that, depending on the valence acquired from previous learning, temporally coded microstimulation activates distinct neural networks and associated behavior.

Key words: amygdaloid complex, electrical microstimulation, fear-conditioning, prefrontal cortex, temporal coding

Introduction

One important question in neuroscience is to unveil how the brain encodes the information it receives from the multitude of sensors spread throughout the human body (Mesulam 1998). Our senses have specialized cells working as transducers that convert physical and/or chemical stimuli into neuronal signals. The first step of encoding can be measured as transmembrane potential changes in the receptor portion of the sensory neurons. Afterwards, these signals have to be transmitted throughout relatively great distances; which poses an engineering challenge that has found its solution in evolution by encoding data digitally (i.e., the action potential) and modulating intensity by Pulse-Frequency-Modulation (Adrian 1964). This latter form of encoding is generally termed Rate Coding; which, in addition to the anatomical specificity of the sensory modality, composes the building blocks of the "language neurons speak" and can be used to either read from or write to a living brain (Olds and Milner 1954; Heynen and Bear 2001; Talwar et al. 2002; O'Doherty et al. 2011). However, as signals propagate from caudal to more rostral neural networks, the encoding processes become increasingly more complex and less localized in terms of anatomy, making rate coding of any individual neuron too imprecise to properly

represent any given attribute (Varela et al. 2001). Although it is still a matter under debate if information is encoded within very small neuronal sets (Quiroga et al. 2005) or distributed among large neuronal populations forming a unique pattern of activation (Rumelhart and McClelland 1986), it is a general consensus that we have just began to fathom the brain's potential to encode information (Rolls and Treves 2011). Time–frequency analyses of LFP recordings, associated with multiunit multielectrode recordings, have contributed much to a compromise solution among the sparse versus distributed coding frameworks (Engel et al. 2001; Buzsaki and Draguhn 2004). An additional complicating factor is that external stimuli processing may even differ from one presentation to another depending on the intrinsic oscillatory activities of the brain at any given moment in time. The time-dependent brain states, which are involved in such top-down modulation, are an important aspect of the sensory-motor integration and may be triggered by the external stimuli itself, generated endogenously or even dynamically formed or modified by learning processes (Engel et al. 2001). Womelsdorf and Fries (2006) have shown that context-dependent phase synchronization of local field potential (LFP) oscillatory activity, from different brain areas, may play a key role in facilitating/modulating sensory input to dynamically activate a motor response for appropriate and flexible sensory-motor coordination (Greenstein et al. 1988; Pavlides et al. 1988; Hyman et al. 2003; Womelsdorf and Fries 2006; Manzur et al. 2013). Therefore, the many oscillators that compose the rhythms of the brain (Buzsáki 2006) may play a key role in synchronizing specific neurons embedded in adjacent or distal neural networks that, nonetheless, compose a relatively precise spatiotemporally organized engram that, in turn, is associated with a perceptual object. The dynamics of such continuous temporal integration, organizing increasingly more complex neural networks in time, may hold the solution of an appropriate sensory-motor response (Singer 1999, 2009).

The importance of quantifying neural synchrony associated to function has stimulated the development of a number of mathematical tools to access time relations of neuronal activity independently of the amplitude of the oscillatory behavior of the resonant networks. These tools have allowed neuroscientists to detect spatial-temporal patterns of network activation to emerge from either stimuli-specific input (Laurent et al. 1996; Normann et al. 2001; Tort et al. 2010) or spontaneous firing, recurring within a scale of seconds-to-minutes, but with millisecond accuracy (Ikegaya et al. 2004). Accordingly, if an estimation of an appropriate temporal bin to account for synchronic discharges, based on the averaged synaptic delay (i.e., 5–10 ms) (Engel and Singer 2001), is thought of as a "bit" of information; the period of oscillation of a theta wave (i.e., ~100–300 ms) (Dehaene and Changeux 2011) of such conceived resonant network would represent a "word" (Dresp-Langley and Durup 2009). In fact, neuronal discharges and external stimuli phase-locked to endogenous theta activity have been shown not only to encode information (Pare et al. 2002; Pare 2003; Buzsaki 2005; Womelsdorf and Fries 2006; Paz et al. 2008; Likhtik et al. 2014) but also to facilitate plastic changes in the underlying neural networks (Greenstein et al. 1988; Pavlides et al. 1988; Hyman et al. 2003). Thus, theoretical models, such as those based on the Adaptive Resonance Theory (Grossberg 1980, 1999) predict a specific binary sequence to be associated with every brain state (Dresp-Langley and Durup 2009) if recorded from key elements within the network. Although, as argued so far, spatial-temporal patterns emerge from recordings of electrophysiological activity during stimuli induced brain states (Singer 1993, 1999, 2009); the microstimulation (μES) of a small neuronal set by binary-coded-words, using the same temporal constrains described above, has not yet been shown to be able to trigger the emergence of specific brain states. Therefore, using a discriminative fear-conditioning paradigm, we evaluated if a trained group of animals could distinguish between different μES binary-coded words (conditioned stimulus—CS); eliciting a conditioned response (CR) only in those cases in which the CS word was previously paired to a footshock (unconditioned stimulus–US). The target of μES was the basolateral amygdaloid complex; chosen not only for its important role in the neurocircuitry of the fear-conditioning paradigm (Blanchard and Blanchard 1972; LeDoux 2003), but also for its polymodal sensory integration and known capability to trigger the arousal of specific brain states (Pare et al. 2002). Finally, 2 h after the last retention test, we evaluated the number of c-Fos immunoreactive labeled (IR) neurons—within neural substrates that were more intimately involved in modulating the behavioral CRs to external stimuli: amygdaloid complex (lateral nuclei—La, central nuclei—Ce, basolateral nuclei—BLA), hypothalamus (VMH and DMD), and prefrontal cortex (IL and PrL) (Pezzone et al. 1992; Smith et al. 1992; LeDoux 2000; Hall et al. 2001; Canteras 2002; Quirk et al. 2003; Vianna et al. 2003; Holahan and White 2004; Knapska et al. 2007; Knapska and Maren 2009)—to establish the activation profiles under 3 possible conditions: (1) μES previously conditioned during training; (2) conditioned to a different μES word; and (3) animals with unpaired μES during training.

Materials and Methods

Subjects

Male Wistar rats (250–310 g) were supplied by the CEBIO-ICB-UFMG vivarium. The animals were allowed free access to food and water and were housed in temperature controlled environment under a 12 h light–dark cycle. Efforts were made to avoid any unnecessary distress to the animals and all experiments were conducted in accordance with NIH guidelines for the care and use of animals. Animal protocols were approved by the Institutional Animal Care and Use Committees at the Universidade Federal de Minas Gerais (CEUA—UFMG; Protocol no. 12/2013), in accordance with CONCEA guidelines defined by the Arouca Act 11.794 under Brazilian Federal Law.

Surgical Procedures

All animals underwent a surgical procedure for implantation of a bipolar stimulation electrode. Electrodes were made of a twisted pair of stainless-steel (0.005 in.), Teflon-coated wires (Model 791400, A-M Systems Inc., Carlsborg, WA, USA). Animals were anesthetized via systemic ketamine/xylazine combination (80 and 15 mg/kg, respectively) and locally at the scalp with lidocaine clorohydrate–epinephrine (2%) solution and then positioned in a stereotaxic frame (Stoelting Co., Wood Dale, IL, USA). Povidine–iodine solution 7.5% for veterinary use (Betadine®) was applied to the scalp for asepsis before the surgical incision. Coordinates for the right basolateral amygdaloid complex (AP = 2.8 mm posterior to bregma, ML = 5.0 mm lateral to bregma, and DV = 8.4 mm ventral to the inner table of the skull.) were derived from the Paxinos and Watson's atlas for rats (Paxinos and Watson 2009). Animals were subject to prophylactic treatment with pentabiotics (19 mg/kg) and flunixin (2.5 mg/kg) to prevent discomfort and infection after surgery. The electrode was fixed onto the skull with zinc cement and soldered to a telephone jack (Model RJ-11), which was fixed to the skull with dental acrylic.

The electrode placement was verified by photomicrographs of histological slices (neutral red staining- ×0.8 magnification) depicting the right basolateral amygdala complex after an electrical current (0.5 mA for 2 s) passed through the bipolar leads (Supplementary Fig. 1). Animals were observed during a 5–7 day postoperative recovery period before initiating the experimental protocol. No animals used in this study presented any signs of surgical complications.

Electrical Microstimulation

The electrical microstimulator set-up consisted of a constant-current isolation unit (Digitimer DS3-Isolated Constant-Current Stimulator) driven by a PC-programmable clocking system, which used the computer's audio output. This system delivered different patterns of temporally coded stimuli (Mesquita et al. 2011). The experiments used 3 different temporal patterns (composed of biphasic square waves, $\lambda = 100$ μs and 25 μA): 6 Hz periodic pattern (IPIs~166.7 ms) and two binary-coded words (10 bins of 10 ms each, applied in time window of 100 ms within a total time of 1 s). In this case maintaining the same number of 6 pulses per second, considering the same parameters: biphasic, $\lambda = 100$ μs and 25 μA square waves but just temporally reorganizing the 6 pulses. These patterns were represented by a sequence of 0's (no-stimulus) and 1's (single-pulse stimulus); namely, (b.1) μES A-pattern (1001111001) and (b.2) μES B-pattern (1110000111).

Conditioning Paradigms

All conditioning paradigms were conducted during the light period of the sleep–awake cycle in 2 different contexts. Preconditioning phases and retention tests for both paradigms occurred in a 30 × 30 × 30 cm transparent acrylic box inside an isolated sound environment scented with 70% ethanol. Conditioning phases were conducted in a different room, to avoid contextual contamination, in a 23 × 23 × 25 cm gray plastic box with gridded floor and a black roof (Insight®), scented with 1% acetic acid.

For the first protocol, a classical conditioning paradigm using a 6-Hz periodic microstimulation pattern as conditioned stimuli was presented 5 times (5 trials) along a 5-s period at the beginning of each trial, applied to the right basolateral amygdaloid complex. The 5 trials were randomly distributed over the duration session (1–3 min). Animals were allowed a 5-min habituation period, once connected to the stimulation apparatus, when placed in either the preconditioning, conditioning, or retention contexts. During the preconditioning phase and retention tests, all groups underwent the same stimulation protocol, which consisted of a 6-Hz periodic pattern of microstimulation. During the conditioning phase an US (footshock, 0.4 mA) was either applied concomitant to the last 2 s of the 5 s microstimulation, paired group ($n = 5$), or pseudorandomly positioned in order to never overlap, within a 20 s minimum lag, to the 5-s microstimulation window, unpaired ($n = 5$) group (Fig. 1A,B). In a second set of experiments, animals were submitted to a discriminative fear-conditioning paradigm, also targeting the right basolateral amygdaloid complex, but the CS was one out of 2 binary-coded words: A-pattern (1001111001) and B-pattern (1110000111). Analogous to the first paradigm, all animals were plugged into the system, introduced into the contexts and allowed for a habituating period of 5 min. During preconditioning and retention tests, both binary-coded words were randomly applied as described in the previous experiment. However, during preconditioning, phase patterns (A- and B-pattern) were individually presented 5 times (10 trials) along a 5-s period at the beginning of each trial. During the conditioning phase, with regard to the unconditioned stimuli (US: 0.4 mA, during last 2 s), animals were divided into 3 distinct groups of stimulation: A-paired and B-unpaired (Red; $n = 6$); A-unpaired and B-paired (Blue; $n = 8$); A-unpaired and B-unpaired (black; $n = 6$). The total number of US, A-pattern or B-pattern presentations was the same (5 times each) for all groups. The criteria of the US paired and unpaired stimulation was the same used in the previous experiment. The retention test consisted of evaluating the conditioned behavior for 3 consecutive days, using only one μES pattern per day as follows: first day B-pattern, second day A-pattern, and last day B-pattern (Fig. 1A,B).

Animal movements were recorded by a video camera set up in front of the box (Supplementary movies 1 and 2). All videos were analyzed offline by a blind examiner. Freezing behavior was defined as no movements, except breathing, for a minimum of 3 s within each 5 s time epoch. Thus, the following 1 min after each μES pattern presentation, during the retention test, was divided into 12 epochs in which a freezing episode either occurred or not (Blanchard and Blanchard 1972; Fanselow and Bolles 1979; Bouton and Bolles 1980; Contarino et al. 2002; Curzon et al. 2009).

Immunofluorescence

The brains from the animals that underwent the discriminative fear-conditioning paradigm were processed for immunofluorescence triple-labeling after the third and last retention test. One and a half hours after the final B-pattern μES, animals from all 3 groups were anesthetized (Urethane 14% w/v; 10 mL/kg) and submitted to a transcardiac perfusion with cold (4°C) phosphate buffer saline (PBS) followed by paraformaldehyde in PBS (PFA, 4% w/v). The brains were removed, post-fixated in PFA and maintained at 4°C. After 24 h, brains were transferred to a sucrose-PBS solution (30% w/v) and maintained at 4°C for the next 3 days. Finally, the brains were frozen in 99% isopentane and maintained at −80°C. Forty micrometer coronal brain sections were obtained (Cryostat 300—ANCAP® Ltd) and stored at −20°C in PBS antifreeze solution [PBS (0,1 M pH 7.2); sucrose (30% w/v); ethylene glycol (30% v/v); polyvinylpyrrolidone (PVP 1% w/v)]. To determine the electrode position, a few slices were selected and stained with neutral red solution [Neutral red (1% w/v); sodium acetate anhydrous (0.3% w/v); acetic acid glacial (0.12% v/v)]. For triple-labeling immunofluorescence, sections were washed 5 times for 5 min each in PBS, incubated with glycine in PBS (0.1 M) for 20 min and then washed 3 times for 5 min each in PBS. After washing, sections were placed in a blocking solution [PBS + Triton X-100 (PBST 0.5% v/v) with normal goat serum (NGS 5% w/v) and bovine serum albumin (BSA 1% w/v)] for 1 h and then incubated with the primary antibody at room temperature for 24 h (rabbit anti-c-Fos 1:2000, Santa Cruz Biotechnology, INC.; mouse anti-NeuN 1:500, Calbiochem®). Each section was then washed 4 times for 5 min in PBS, followed by a 1 h incubation period at room temperature with the secondary antibody (Alexa Fluor® 488 goat anti-rabbit 1:500, Molecular Probes®; Alexa Fluor® 647 goat anti-mouse 1:500, Molecular Probes®). Each section was then washed 6 times for 5 min each in PBS and incubated for 15 min with 4',6-diamidino-2-phenylindole (DAPI) (1:10000). Finally, the sections were washed 3 times for 10 min each in PBST and mounted on micro glass slides (Superfrost® Plus) embedded in aqueous nonfluorescing mounting gel (Hidromount TM).

c-fos Immunoreactive Labeling (IR) Neurons Analyses

To analyze c-fos expression the number of immunoreactive labeling neurons was counted. The microstimulation electrodes

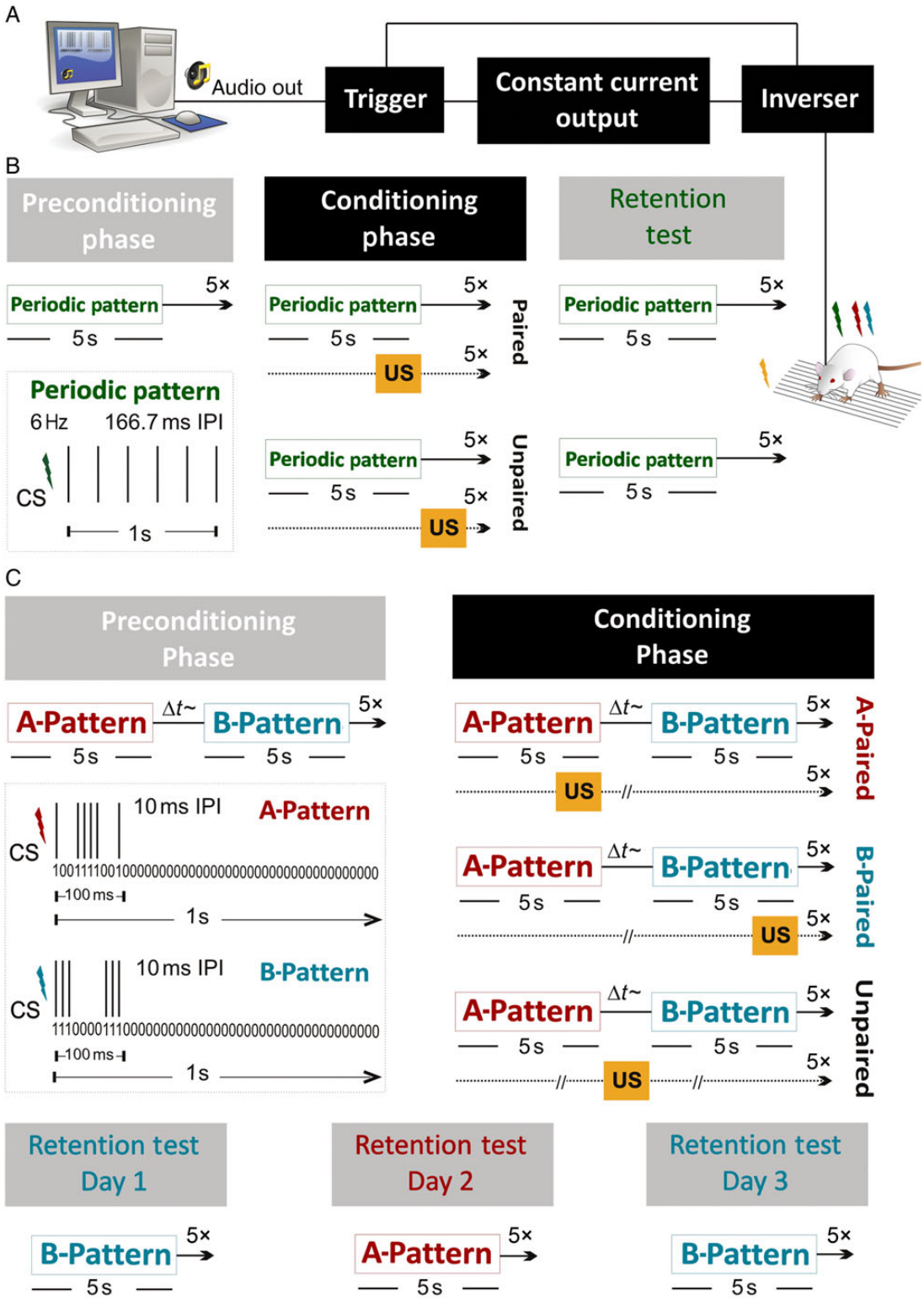

Figure 1. Experimental setup and conditioning parameters. (*A*) Experimental setup. (*B*) Classic fear-conditioning paradigm. The 6-Hz periodic pattern of microstimulation was applied 5 times randomly over the sessions, which were paired or unpaired with a footshock US during the conditioning phase. (*C*) Discriminative fear-conditioning paradigm. It was assessed if animals could discriminate between 2 μES binary-coded words: A-pattern and B-pattern. Three groups of animals were submitted to the conditioning phase under different pairing associations between the μES and the US: A-paired and B-unpaired (red); A-unpaired and B-paired (blue); A-unpaired and B-unpaired (black). Conditioned behavior was evaluated for 3 consecutive days using the same μES pattern per day; respectively, *b*—*a*—*b*.

were positioned at the right amygdaloid complex. Images were taken from the left amygdaloid complex covering the lateral and central nucleus; from the right and left amygdaloid complex basolateral nucleus and from the dorsomedial and ventromedial hypothalamic nuclei. Furthermore, prefrontal-cortex images were taken covering Prelimbic and Infralimbic

areas (3.72–3.00 mm AP). Three to 5 sections for each area were imaged and later averaged to obtain a single value per region of interest (ROI). Images were acquired on a fluorescence microscope Axio Imager.M2—Zeiss system with ×20/0.5 and ×40/0.75 objectives using Carl Zeiss Axiovision 4.8 software to create images. Exposure time was set with the same values for all data collected. For each ROI, images were separately acquired for c-Fos, NeuN, and DAPI staining using specific filters sets compatible with the excitation–emission profiles of each fluorescent dye. Raw files were processed by the z-stack method (minimum ~4 µm optical stacks collected) and mounted images were analyzed in Image-J software (http://rsbweb.nih.gov/ij/). The background auto-fluorescence was subtracted by applying the same threshold filter to all images and then the number of c-Fos/NeuN-positive staining was determined by colocalization—Image-J plugin (Costes et al. 2004). Cells were defined as particles at least 30 to 40 µm^2. Total neurons NeuN-positive staining was determined and the number of c-Fos/NeuN-positive staining was normalized to the total neurons, expressed as percentage of c-Fos/NeuN-positive staining. Finally, images were digitally merged and contrast or brightness was similarly adjusted for each best-case result showed.

Statistical Analysis

All data are presented as means ± SEM. The approximation to the normal distribution was confirmed by the Kolmogorov–Smirnov test. Statistical comparisons were made using one-way or 2-way repeated-measures analysis of variance, when appropriate followed by Bonferroni post hoc test in accordance with the coefficient of variation. For some supplementary analyses, statistical comparisons were made using χ^2 test and Kolmogorov–Smirnov test (K–S 2-sample test). Values of $P < 0.05$ were considered statistically significant. Data were analyzed using GraphPad Prism 6.0 Software and MATLAB, The Mathworks, Natick, USA.

Results

Classical Fear-Conditioning Paradigm with a 6-Hz Periodic Microstimulation Pattern

An experimental protocol was designed to assure 2 prime aspects of the fear-conditioning paradigm (Fig. 1A,B): the µES used would not in itself induce an aversive behavioral response (neutral stimuli—NS) and that once paired with a US, the µES would then become a CS capable of eliciting a CR.

A potential setback of using the 6 Hz ES comes from the evidence that such stimuli might cause abnormal/pathological network activity. Accordingly, the 6-Hz model of epilepsy, proposed by Toman ~60 years ago (Toman 1951), has just recently regained notoriety as a possible acute animal model for drug resistant epileptic seizures (Barton et al. 2001). Nevertheless, the µES parameters used in this work were specifically chosen to avoid self-triggered abnormal behavioral outcome. First, the µES (25 µA) is a thousand times smaller than the 32 mA used in the beforementioned 6 Hz model and over 10 times smaller than other low-current ES triggered epilepsy animal models, e.g., the Electrical Kindling of the Amygdala (Racine 1972). The pulse width fixed at a 100 µs biphasic square wave is quite smaller than the 1 ms duration pulse used for seizure induction. In addition, the Electrical Kindling model uses a 60-Hz stimulation protocol for several seconds; our stimulation protocol delivers 6 pulses during 1 s, presented for only 5 times at each session. The total number of stimulation sessions was also inferior to what would be necessary to induce behavioral alterations in the kindling model. In summary, this first experimental group was designed to assure that the µES used did not promote, in itself, any behavioral outcome such as myoclonic jerks, minor twitching, freezing, or other visible motor responses.

According to the results, a 6-Hz periodic µES pattern, with constant interpulse intervals, applied to the amygdaloid complex, satisfied the before-mentioned criteria; inducing a higher CS-triggered freezing behavior only in the group in which the initial NS was paired to the US (Fig. 2A; Supplementary Movie 1) ($n = 5$ per group, $F_{1,8} = 7.415$, $^{**}P < 0.01$). In addition, there was no observable behavioral outcome from the nonpaired group after stimuli was applied.

Discriminative Fear-Conditioning Paradigm with 2 Different Binary-Coded Words

Maintaining the same number of 6 pulses per second, the next set of experiments used 2 different binary-coded words (10 bins of 10 ms each) represented here by a sequence of 0's (no-stimulus) and 1's (single-pulse stimulus): µES A-pattern(1001111001) and µES B-pattern (1110000111). Thus, 3 groups of animals were used, differing only on the choice of which µES pattern was to be paired to the US during conditioning phase (Fig. 1A,C): A-paired, B-paired, or unpaired to both patterns. Following the conditioning phase, during 3 consecutive days, the retention test consisted of presenting a daily µES pattern, for all animals, according to the following sequence: B-pattern, A-pattern, and B-pattern µES. As expected, during the preconditioning phase, neither A-pattern nor B-pattern triggered any significant aversive behavior. During the first day of retention test, when µES B-pattern was used as CS, only the B-paired group displayed a proper CR behavior. However, during the second day, when all groups were subject to the µES A-pattern, the B-paired group that increased freezing behavior the day before ceased to respond and only the A-paired group showed a proper CR behavior. At the third day of testing, groups resumed responding as they did in the first day of the retention test phase (Fig. 2B; Supplementary Fig. 2; Supplementary Movie 2). Also, the CR during the retention test was statistically different from the preconditioning phase only for the groups in which the retention test µES pattern was the same as the one paired during the conditioning phase (Fig. 2C,D; Supplementary Fig. 2). In the control group, the µES failed to induce a CR in any of the 3 consecutive retention tests (Fig. 2B; Supplementary Fig. 3). (A-paired $n = 6$; B-paired $n = 8$; Unpaired $n = 6$, $F_{8,68} = 5.572$, $^{*}P < 0.05$; $^{**}P < 0.001$; $^{***}P < 0.0001$).

The CR for all groups, during the 3 retention tests, was also quantified in terms of the probability of the first freezing event to occur within the first time epoch after stimuli presentation. Both first freezing event histogram and discrete probability distribution estimation showed statistically significant profiles (Supplementary Fig. 3) that corroborate previously shown data analysis from the last paragraph (Fig. 2B).

Profiles of Amygdaloid-Hypothalamic and Amygdaloid-Prefrontal Circuitry Based on C-Fos Immunoreactive Labeling Neurons

The hypothesis being tested by the neural activity marker protocol (c-Fos labeling) is that the µES, using a previously conditioned binary-coded word, would trigger a brain state that would, in turn, modulate the appropriate neural substrates involved in the sensory-motor integration of the fear-conditioning paradigm. Conversely, if the pattern not associated with the CR

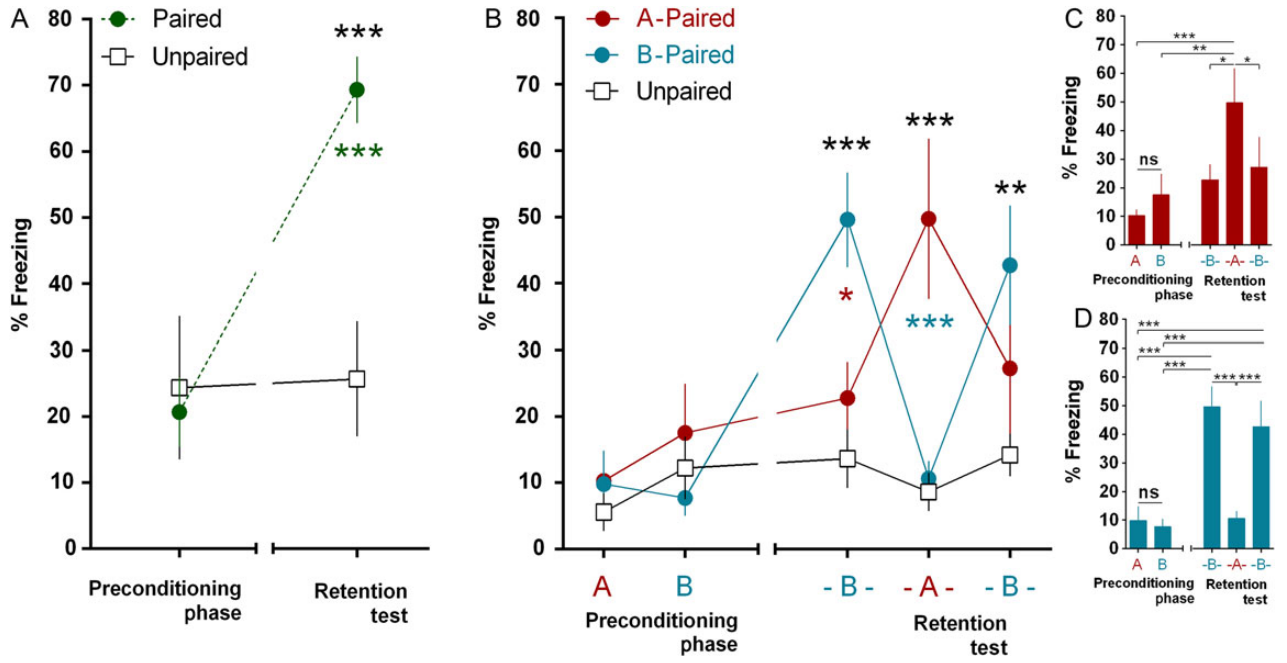

Figure 2. Evaluation of the CR to amygdaloid complex µES. (*A*) Classic fear-conditioning paradigm with periodic µES. Paired group showed significant freezing on retention test compared with the preconditioning phase and unpaired group ($n = 5$ per group, $F_{1,8} = 7.415$, $P < 0.026$; $^{**}P < 0.01$). (*B*) Discriminative fear-conditioning paradigm. A proper CR was observed on day 1 only for the B-paired group, on day 2 only for the A-paired group and resumed first day like behavior on day 3. (*C*,*D*) Paired groups showed significant freezing on the retention test when compared with the preconditioning phase and unpaired patterns (A-Paired $n = 6$; B-Paired $n = 8$; Unpaired $n = 6$, $F_{8,68} = 5.572$, $P < 0.0001$; $^{*}P < 0.05$; $^{**}P < 0.01$; $^{***}P < 0.001$). Percentage freezing quantified during protocols as mean ± SEM.

evocation were used, one would expect the activation of brain substrates best known to be involved in modulating sensory valences and/or evaluating different contingencies. The dueling cross-modulation between prefrontal cortex and the temporal-lobe substrates has been shown to be an important factor inhibiting unsuitable responses from non-associated stimulus (Quirk et al. 2003; Likhtik et al. 2014). Thus, after the last retention test presentation with B-pattern µES, the number of c-Fos^{+}/NeuN immunoreactive labeling (IR) neurons was used to compare activation profiles of amygdaloid-hypothalamic and amygdaloid-prefrontal circuitry for all 3 animal groups. The mechanical lesion due to electrode implantation partially compromised c-Fos IR quantification of ipsilateral AMG subnuclei (Supplementary Fig. 4). The groups show very distinct patterns of c-Fos IR depending on the stimulation pattern used. The B-paired group had stronger c-Fos IR in hypothalamic (Fig. 3; Supplementary Figs 5 and 6) (A-paired, red $n = 6$; B–paired, blue $n = 7$; Unpaired, black $n = 6$. DMD, $F_{2,16} = 13.85$, $^{**}P < 0.01$, $^{***}P < 0.001$. VMH, $F_{2,16} = 6.631$, $^{*}P < 0.05$), and amygdaloid subnuclei (Fig. 4*A*–*H*) (A-paired, red $n = 6$; B-paired, blue $n = 7$; Unpaired, black $n = 6$. La, $F_{2,16} = 5.245$. Ce, $F_{2,16} = 8.515$, $^{**}P < 0.01$. BLA, $F_{2,16} = 3.050$, $^{*}P < 0.05$) while the A-paired group favored prefrontal-cortex activation (Fig. 4*I*–*N*; Supplementary Figs 5 and 6) (A-paired, red $n = 6$; B-paired, blue $n = 7$; Unpaired, black $n = 6$. PrL, $F_{2,16} = 10.20$, $^{**}P < 0.01$. IL, $F_{2,16} = 8.7$, $^{**}P < 0.001$). Furthermore, there were no statistical differences between A-paired group c-Fos IR in hypothalamic nuclei when compared with the unpaired group and neither for the B-paired group c-Fos IR in prefrontal cortex when compared with the unpaired group (Figs 3 and 4).

The c-Fos IR versus freezing Pearson Correlation data depicted in Supplementary Figure 5 show a significant ($r = 0.74$, $P < 0.05$) correlation value for the DMD nuclei. The only negative correlations are from the prefrontal cortex areas (PrL, $r = -0.44$, $P = 0.11$ and IL, $r = -0.39$, $P = 0.16$); with amygdaloid (La, $r = 0.44$, $P = 0.11$; Ce $r = 0.48$, $P = 0.08$ and BLAe $r = 0.29$, $P = 0.29$) and VMH ($r = 0.31$, $P = 0.29$) areas showing positive correlation. Although the *P* values from PrL and IL did not reach the significance criteria convention, the fact that these were the only areas to show negative c-Fos IR versus freezing correlation corroborates Figures 3 and 4 results; thus, reinforcing our main hypothesis of differential network recruitment.

Discussion

The present results show that animals were able to distinguish between the preestablished A and B temporal patterns depending on the previous experienced paradigm to which they were subject during the conditioning phase. The behavioral data and the IR data coherently show that only the paired binary-coded word properly triggered a fear response, recruiting the amygdalo-hypothalamic circuitry involved in downstream sympathoexcitatory activation (Colpaert and Wiepkema 1976; Pezzone et al. 1992; Hall et al. 2001; de Oliveira et al. 2013). The A-paired group recruited the prefrontal cortex after B-pattern stimulation, showed unaltered hypothalamic labeling when compared with controls and did not present a significant aversive response, suggesting a brain state directed toward evaluating different contingencies (Fig. 5) (Quirk et al. 2003).

Several studies have shown that specific spatial-temporal patterns emerge within neural ensembles due to contextual or sensory stimuli (Laurent et al. 1996; Normann et al. 2001; Warren et al. 2001; Ikegaya et al. 2004). Nevertheless, most of the experimental designs have privileged a one-way street in which temporal coding is passively recorded after eliciting a specific brain state. This is the first report that has shown that a temporally coded µES, targeted at a single area, is able to differentially trigger specific circuits associated with distinct behavioral outcomes. In fact, the aversive nature of the behavioral response and neural

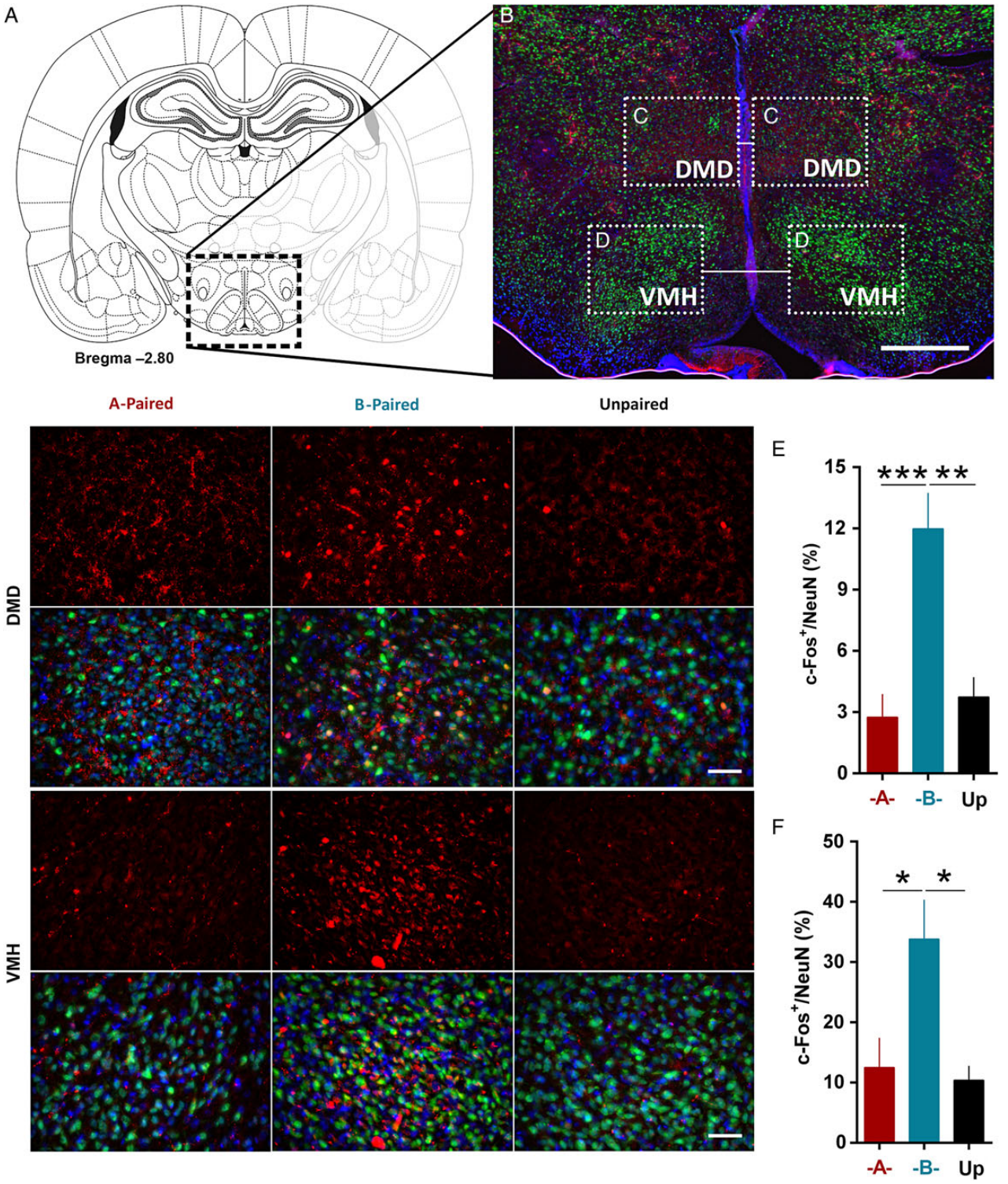

Figure 3. Hypothalamus immunoreactive triple-labeling after the last retention test presentation with B-pattern μES. (*A*) Representative diagram of the section. (*B*) Typical triple-labeling immunofluorescence (NeuN—green, c-Fos—red and DAPI—blue) showing ROIs; (*C*) Dorsomedial—DMD, (*D*) Ventromedial—VMH hypothalamic nuclei; ×5 magnification; scale bar 1 mm. Lower left panel: typical triple-labeling immunofluorescence for all groups, depicting the VMH and DMD; ×40 magnification; scale bar 100 μm. (*E*,*F*) Column graphs showing the mean number for c-Fos/neuN immunoreactive labeling (IR) neurons in each specific ROIs. The B-paired group showed significant higher c-Fos$^+$/NeuN IR when compared with the A-paired and Unpaired groups. (*a*-Paired $n = 6$; *b*-Paired $n = 7$; Unpaired $n = 6$, DMD, $F_{2,16} = 13.85$, $p = 0.003$; $^{**}P < 0.01$, $^{***}P < 0.001$. VMH, $F_{2,16} = 6.631$, $p = 0.008$; $^{*}P < 0.05$). All data presented as mean ± SEM.

ensembles recruited in the experimental paradigm were dependent on the preassociated μES temporal patterns. Other studies have used μES to force neuronal synchrony and/or temporal correlation among different neural networks in order to elicit appropriate behavioral responses (Quinkert et al. 2010; O'Doherty et al. 2012; Manzur et al. 2013; Medeiros et al. 2014). Of particular

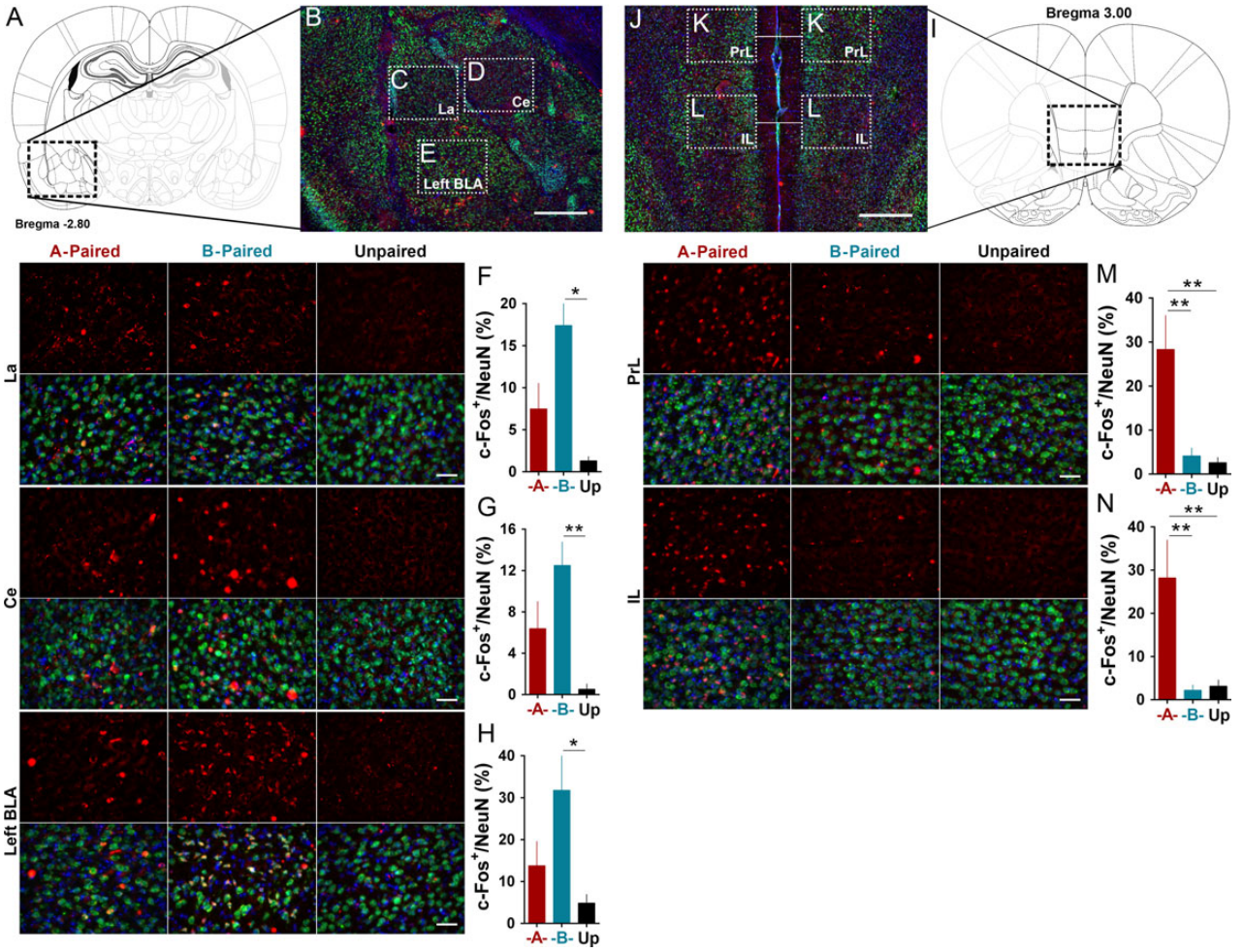

Figure 4. Amygdaloid complex and prefrontal-cortex immunoreactive triple-labeling after the last retention test presentation with B-pattern µES. (*A*,*I*) Representative diagram of the section. Typical triple-labeling immunofluorescence (NeuN—green, c-Fos—red and DAPI—blue) showing ROIs; (*B*) Amygdaloid complex: (*C*) Lateral (La), (*D*) Central (Ce), (*E*) Left basolateral (Left BLA) nuclei; (*J*) Prefrontal cortex: (*K*) Prelimbic (PrL), (*I*) Infralimbic (IL); ×5 magnification; scale bar 1 mm. Typical triple-labeling immunofluorescence for all groups, depicting the La, Ce, and left BLA (lower left panel) and the PrL and IL (lower right panel); ×40 magnification; scale bar 100 µm. Column graphs showing the mean number for c-Fos$^+$/NeuN immunoreactive labeling (IR) neurons in each specific ROIs; (*F*,*G*,*H*) B-paired group showed significant higher c-Fos$^+$/NeuN IR neurons when compared with the Unpaired group for all amygdaloid nuclei (A-Paired $n = 6$; B-Paired $n = 7$; Unpaired $n = 6$. La, $F_{2,16} = 5.245$, $P = 0.017$. Ce, $F_{2,16} = 8.515$, $p = 0.003$. BLA, $F_{2,16} = 4.466$, $P = 0.028$; $^*P < 0.05$, $^{**}P < 0.01$). (*M*,*N*) A-paired group showed significant higher c-Fos$^+$/NeuN IR neurons when compared with either B-paired and Unpaired groups for all prefrontal ROIs. (A-Paired $n = 6$; B-Paired $n = 7$; Unpaired $n = 6$. PrL, $F_{2,16} = 10.20$, $P = 0.001$; $^{**}P < 0.01$. IL, $F_{2,16} = 8.7$, $P = 0.002$; $^{**}P < 0.001$). All data presented as mean ± SEM.

interest to our work, Manzur et al. (2013) have shown that specific µES synchronization features, among electrodes positioned in different brain areas, may guide an appropriate response in a behavioral discrimination task. Although the work does not apply the specific temporal pattern arrangements of µES like the ones used here, it does suggest that temporal synchronization of multi-electrode stimulation may be an unexplored new dimension for brain–machine interface feedback (Manzur et al. 2013). In addition, Quinkert et al. (2010) have shown that the temporal organization of ES has an effect on behavioral arousal and several endogenous oscillators, i.e., spectral distribution of the EEG, when applied to a polymodal associative area (Quinkert et al. 2010).

One important consideration, regarding the very nature of the temporal sequences of the A and B-word patterns, must be debated in further detail. Within a 10 bin 100 ms word, both patterns begin and end with stimuli, leaving 8 free-spots to receive 4 stimuli out of a total of 6. Thus, the combinatory arrangement of $C_{8,4}$ will give a total of 70 possible combinations to test for differences in time-coding under such framework. The first basic consideration to address is if, even in the best-case scenario of several "bit-shifts", making the temporal sequences as different as possible, the underlying neural networks are able to distinguish between different temporally coded pattern-specific stimuli. However, by choosing the A and B-word patterns with such high-enough number of "bit-shifts", the µES-words could be interpreted as having one (A-word) or 2 (B-word) high-frequency "clusters". It is pertinent to highlight the distinction between the formerly named high-frequency "clusters", composed of 3 or 4 consecutive pulses at 10-ms interpulse intervals, and a high-frequency 100 Hz stimulation burst, which usually has more than 1 s duration (>100 pulses). The known effects of high-frequency stimulation bursts may not apply to such "very short" number of stimuli, especially considering the µES settings at 25 µA. In fact, using the PTZ animal model of seizure induction, previously published work from our laboratory showed that 4 consecutive stimuli (600 µA to the amygdaloid complex) at 10 ms interpulse intervals (control group with 100 Hz

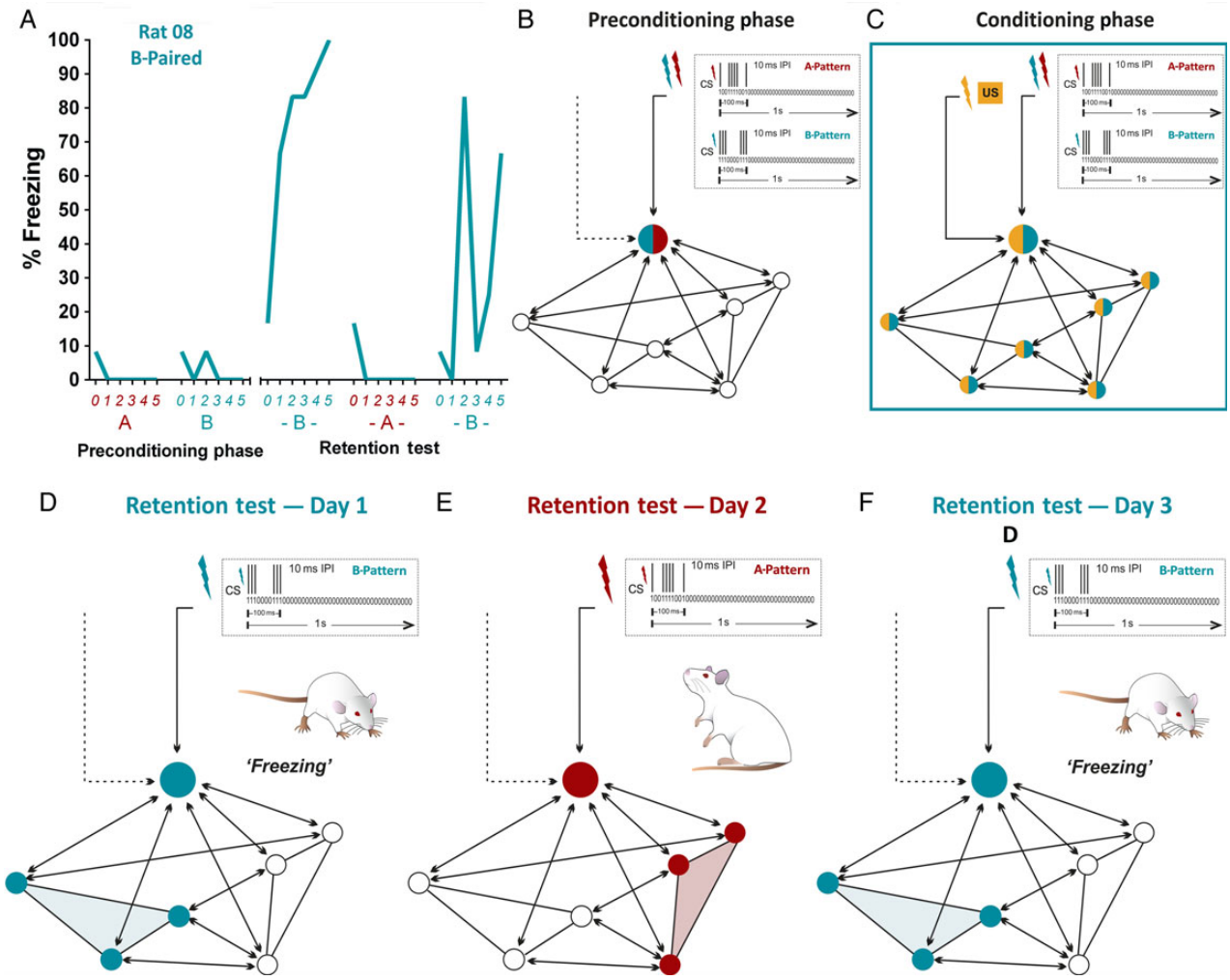

Figure 5. Discriminative fear-conditioning neural network based on adaptive resonant models. (*A*) Individual freezing responses per each trial for rat #8 showing that μES pattern-B, applied to the right basolateral amygdaloid complex, was distinguishable from μES pattern-A as evidenced by higher freezing behavior during retention test days 1 and 3. (*B*) The preconditioning phase did not elicit freezing behavior, thus no specific brain state emerged from μES. (*C*) During the conditioning phase, a specific temporal pattern (i.e., μES pattern-B) changed amygdaloid-hypothalamic reverberating networks connectivity facilitating downstream aversive response. (*D–F*) Emergence of different brain states during the discriminative protocol recruiting specific resonant networks depending on the binary-coded word previously programed during the conditioning phase (blue: amygdaloid-hypothalamic reverberation and red: amygdaloid-prefrontal-cortex reverberation).

high-frequency cluster) had no effect on ictogenesis, while periodic stimulation was proconvulsive and nonperiodic (pseudo-random) was anticonvulsive (Cota et al. 2009). This evidence strengthens the argument that the temporal reorganization of ES alone, and not the "high-frequency cluster", would have a key importance on the neural dynamics of the ictogenic process. In addition, regarding the current stimulation paradigm, if the 2 μES words presented in our work were processed by the underlying neural circuit as formed by one (A-word) or 2 (B-word) high-frequency "clusters", it would be more reasonable to expect a potentiated CR of the A-word conditioned animals when presented to a B-word during the test phase; which was not the case. Also, the B-word conditioned animals, when presented to an A-word during the test phase, should have had a less efficient CR, but still higher than nonpaired controls; also not supported by our findings (Fig. 2*B*; Supplementary Figs 2 and 3; Movie 2). The much more complex question that arises from such conditions, pertaining to the neurophysiology of temporal coding, is how many bit-shifts would be necessary in order to implicate in different neural processing of the stimulation patterns; this is currently under investigation.

One possible interpretation of our results is that temporally coded μES, targeted at strategic nuclei, may favor the coupling of specific network oscillators throughout the brain; thus leading to distinct behavioral outputs (Fig. 5). Our results show that the facilitated downstream activation of amygdaloid-hypothalamic connections, substrates known to be involved in the fear-response, are dependent on the temporal organization of neuronal discharge (Figs. 3 and 4; Supplementary Fig. 6). If time-independent plastic changes in synaptic modulation were the only factor involved in the associative learning paradigm, both μES patterns would have evoked similar circuitry activation. However, if the flow of the before-mentioned downstream activation were a result of plastic changes modulating the coupling of several network oscillators, only a specific pattern of μES would trigger the proper arrangement for hypothalamic recruitment. Conversely, if the pattern is not recognized, but similar to other patterns with associated emotional valence, other neural substrates should be recruited in order to properly process amygdaloidal activation, e.g., prefrontal cortex (Fig. 4*I–N*; Supplementary Fig. 6) (Likhtik et al. 2014). Several data showing the role of prefrontal cortex in learned aversive response support such a claim

(Quirk et al. 2003; Moscarello and LeDoux 2013). Altogether, our results show that the behavior versus network activation (c-Fos$^+$/NeuN IR results) correlation profiles are dynamically elicited by the temporal arrangement features of the μES patterns.

Nevertheless, some explanatory considerations regarding our c-Fos$^+$/NeuN IR neurons need to be made. The activity maps obtained from c-Fos labeling are dependent on a quite uniform temporal window that involves increased second-messenger signaling within the neuron (e.g., intracellular Ca^{+2}), caused by membrane depolarization and/or receptor stimulation, followed by kinase activation. The protein levels peak at roughly 30–90 min after the neurons have been recruited and accumulate inside the cell for a short period of time thereafter. In summary, the c-Fos mapping methodology most commonly used throughout literature consists of processing the tissue ~2 h after an experimental trigger is delivered (Miller et al. 1984; Knapska and Maren 2009). In addition, many researchers have investigated the neural substrates involved in the classical conditioning paradigm by employing c-Fos mapping techniques (Pezzone et al. 1992; Smith et al. 1992; Hall et al. 2001; Holahan and White 2004; Knapska et al. 2007; Knapska and Maren 2009). The correlation between c-Fos labeling and freezing is compromised not only by the dispersion of data, intrinsic to the behavioral evaluation of the conditional response, but also to the complexity of neural processing under the fear-conditioning paradigm (Supplementary Fig. 5) (Holahan and White 2004). However, the activation of specific hypothalamic nuclei directly involved in defensive behaviors (i.e., DMD) have been shown to have high correlation with freezing behavior (Canteras 2002) (Supplementary Fig. 5). On the other hand, substrates processing or modulated by learning, memory fixation, consolidation, and recovery may not have such clear-cut activation profiles to the CR behavioral marker. Accordingly, the lateral and central amygdaloidal nuclei activation may occur during both CS and US presentation, especially evident after the US, while BLA labeling is primarily attributed to CS presentation (Pezzone et al. 1992; Hall et al. 2001). Nevertheless, our results corroborate these findings once c-Fos$^+$/NeuN BLA labeling was considerably higher than lateral and central amygdaloidal nuclei activation after CS was presented (Supplementary Fig. 6). Furthermore, a potential limitation imposed by methodology is the spatial resolution of areas activated by the targeted ES. Although the bipolar stainless-steel electrodes were designed with a small exposed tip and stimulated with low intensity currents (25 μA) to increase target specificity, no further claim may be made as to whether passage fibers or other amygdaloidal subnuclei could also have been activated, thus yielding to increased variability. It is also important to highlight that different stimulation methodologies (e.g., optogenetics targeted at BLA cell bodies), considered much more specific in terms of neuronal activation, also lead to high variability in behavior outcome quantification (Stuber et al. 2012).

The c-Fos mapping of the B-Paired group may also reflect the activation of substrates involved in an on-going process of extinction (Knapska et al. 2007); considering that the group was previously stimulated, on day 1, with the same μES pattern. In fact, although Figure 2 does not characterize a typical process of memory extinction (Supplementary Fig. 3) depicting a temporally structured freezing-response analysis suggests it is present. However, since the extinction process requires the reactivation of circuits triggered by the CS in a nonreinforced session (Quirk 2002; Knapska and Maren 2009), the reverberation of circuits initiated by the temporally coded word pattern are a necessary aspect of extinction. In other words, the extinction process does not preclude reverberation of the encoded information triggered by B-Pattern μES; in fact, it is a required step for extinction. Therefore, even if the circuit activation maps reflect concomitant processes, the overall conclusion regarding the ability to distinguish between differently temporally coded μES patterns is still valid. Moreover, there were only 2 nonreinforced sessions for the B-Paired group (i.e., the A-Pattern μES day 2 retention test was not effective in eliciting a fear-expression response, thus not likely to involve neural substrates associated with the extinction process).

Our results corroborate the hypothesis that the temporal pattern of activation of a strategically positioned neuron within the network may dynamically drive the complex coupling of the myriad of oscillatory microcircuits involved in the emergence of a brain state (Fig 5). The frequency bands of LFPs have been associated with such myriad of oscillatory circuits—the lower the frequency the bigger the circuit (Rey et al. 2014)—that, in turn, may encode information by coupling/synchronizing elements of the underlying neural network among each other within specific time windows. Such temporal organization of network activity, modulating the flux of information throughout neuronal ensembles, has been proposed as a form of phase encoding (Varela et al. 2001). This premise has been experimentally observed in situations where the emergence of attentional states, although not changing the overall discharge rate of specific neurons within the ensemble, synchronized neuronal discharge to LFP oscillations at specific phase lags (Engel et al. 2001)

In summary, we concluded that a single-channel μES electrode placed at the amygdaloid complex can recruit different underlying circuits and elicit different behaviors simply by temporally reorganizing the 6 pulses within a binary-coded word. Thus, this asynchronous serial communication interface is able to trigger the emergence of different brain states depending on the binary-coded word previously programed during the training of the associative memory.

Supplementary Material

Supplementary material can be found at: http://www.cercor.oxfordjournals.org/.

Funding

This work was supported by Fundação de Amparo à Pesquisa do Estado de Minas Gerais (CBB-APQ-02290-13 and TEC-APQ-01084-13), Coordenação de Aperfeiçoamento de Pessoal de Nível Superior (MINCYT 0951/2013) and Conselho Nacional de Desenvolvimento Científico e Tecnológico (476681/2012-0, 470532/2012-2 and 306767/2013-9).

Notes

We are grateful to CNPq, FAPEMIG, CAPES, and PRPq/UFMG, for financial support. *Conflict of Interest*. None declared.

References

Adrian EDAB. 1964. The basis of sensation. The action of the sense organs. New York, London: Hafner Publishing Co.

Barton ME, Klein BD, Wolf HH, White HS. 2001. Pharmacological characterization of the 6 Hz psychomotor seizure model of partial epilepsy. Epilepsy Res. 47:217–227.

Blanchard DC, Blanchard RJ. 1972. Innate and conditioned reactions to threat in rats with amygdaloid lesions. J Comp Physiol Psychol. 81:281–290.

Bouton M, Bolles R. 1980. Conditioned fear assessed by freezing and by the suppression of three different baselines. Anim Learn Behav. 8:429–434.

Buzsaki G. 2005. Theta rhythm of navigation: link between path integration and landmark navigation, episodic and semantic memory. Hippocampus. 15:827–840.

Buzsáki G. 2006. Rhythms of the brain. Oxford, New York: Oxford University Press.

Buzsaki G, Draguhn A. 2004. Neuronal oscillations in cortical networks. Science. 304:1926–1929.

Canteras NS. 2002. The medial hypothalamic defensive system: hodological organization and functional implications. Pharmacol Biochem Behav. 71:481–491.

Colpaert FC, Wiepkema PR. 1976. Brief communication ventromedial hypothalamus: fear conditioning and passive avoidance in rats. Physiol Behav. 16:91–95.

Contarino A, Baca L, Kennelly A, Gold LH. 2002. Automated assessment of conditioning parameters for context and cued fear in mice. Learn Mem. 9:89–96.

Costes SV, Daelemans D, Cho EH, Dobbin Z, Pavlakis G, Lockett S. 2004. Automatic and quantitative measurement of protein–protein colocalization in live cells. Biophys J. 86:3993–4003.

Cota VR, Medeiros Dde C, Vilela MR, Doretto MC, Moraes MF. 2009. Distinct patterns of electrical stimulation of the basolateral amygdala influence pentylenetetrazole seizure outcome. Epilepsy Behav. 14(Suppl 1):26–31.

Curzon P, Rustay NR, Browman KE. 2009. Cued and contextual fear conditioning for rodents. In: Buccafusco JJ, editors. Methods of behavior analysis in neuroscience. 2nd ed. Boca Raton (FL).

de Oliveira AR, Reimer AE, Reis FM, Brandao ML. 2013. Conditioned fear response is modulated by a combined action of the hypothalamic-pituitary-adrenal axis and dopamine activity in the basolateral amygdala. Eur Neuropsychopharmacol. 23:379–389.

Dehaene S, Changeux JP. 2011. Experimental and theoretical approaches to conscious processing. Neuron. 70:200–227.

Dresp-Langley B, Durup J. 2009. A plastic temporal brain code for conscious state generation. Neural Plast. 2009:482696.

Engel AK, Fries P, Singer W. 2001. Dynamic predictions: oscillations and synchrony in top-down processing. Nat Rev Neurosci. 2:704–716.

Engel AK, Singer W. 2001. Temporal binding and the neural correlates of sensory awareness. Trends Cogn Sci. 5:16–25.

Fanselow MS, Bolles RC. 1979. Naloxone and shock-elicited freezing in the rat. J Comp Physiol Psychol. 93:736–744.

Greenstein YJ, Pavlides C, Winson J. 1988. Long-term potentiation in the dentate gyrus is preferentially induced at theta rhythm periodicity. Brain Res. 438:331–334.

Grossberg S. 1980. How does a brain build a cognitive code? Psychol Rev. 87:1–51.

Grossberg S. 1999. The link between brain learning, attention, and consciousness. Conscious Cogn. 8:1–44.

Hall J, Thomas KL, Everitt BJ. 2001. Fear memory retrieval induces CREB phosphorylation and Fos expression within the amygdala. Eur J Neurosci. 13:1453–1458.

Heynen AJ, Bear MF. 2001. Long-term potentiation of thalamocortical transmission in the adult visual cortex in vivo. J Neurosci. 21:9801–9813.

Holahan MR, White NM. 2004. Amygdala c-Fos induction corresponds to unconditioned and conditioned aversive stimuli but not to freezing. Behav Brain Res. 152:109–120.

Hyman JM, Wyble BP, Goyal V, Rossi CA, Hasselmo ME. 2003. Stimulation in hippocampal region CA1 in behaving rats yields long-term potentiation when delivered to the peak of theta and long-term depression when delivered to the trough. J Neurosci. 23:11725–11731.

Ikegaya Y, Aaron G, Cossart R, Aronov D, Lampl I, Ferster D, Yuste R. 2004. Synfire chains and cortical songs: temporal modules of cortical activity. Science. 304:559–564.

Knapska E, Maren S. 2009. Reciprocal patterns of c-Fos expression in the medial prefrontal cortex and amygdala after extinction and renewal of conditioned fear. Learn Mem. 16:486–493.

Knapska E, Radwanska K, Werka T, Kaczmarek L. 2007. Functional internal complexity of amygdala: focus on gene activity mapping after behavioral training and drugs of abuse. Physiol Rev. 87:1113–1173.

Laurent G, Wehr M, Davidowitz H. 1996. Temporal representations of odors in an olfactory network. J Neurosci. 16: 3837–3847.

LeDoux J. 2003. The emotional brain, fear, and the amygdala. Cell Mol Neurobiol. 23:727–738.

LeDoux JE. 2000. Emotion circuits in the brain. Annu Rev Neurosci. 23:155–184.

Likhtik E, Stujenske JM, Topiwala MA, Harris AZ, Gordon JA. 2014. Prefrontal entrainment of amygdala activity signals safety in learned fear and innate anxiety. Nat Neurosci. 17:106–113.

Manzur HE, Alvarez J, Babul C, Maldonado PE. 2013. Synchronization across sensory cortical areas by electrical microstimulation is sufficient for behavioral discrimination. Cereb Cortex. 23:2976–2986.

Medeiros DC, Oliveira LB, Mourao FA, Bastos CP, Cairasco NG, Pereira GS, Mendes EM, Moraes MF. 2014. Temporal rearrangement of pre-ictal PTZ induced spike discharges by low frequency electrical stimulation to the amygdaloid complex. Brain Stimul. 7:170–178.

Mesquita MB, Medeiros Dde C, Cota VR, Richardson MP, Williams S, Moraes MF. 2011. Distinct temporal patterns of electrical stimulation influence neural recruitment during PTZ infusion: an fMRI study. Prog Biophys Mol Biol. 105: 109–118.

Mesulam MM. 1998. From sensation to cognition. Brain. 121(Pt 6):1013–1052.

Miller AD, Curran T, Verma IM. 1984. c-fos protein can induce cellular transformation: a novel mechanism of activation of a cellular oncogene. Cell. 36:51–60.

Moscarello JM, LeDoux JE. 2013. Active avoidance learning requires prefrontal suppression of amygdala-mediated defensive reactions. J Neurosci. 33:3815–3823.

Normann RA, Warren DJ, Ammermuller J, Fernandez E, Guillory S. 2001. High-resolution spatio-temporal mapping of visual pathways using multi-electrode arrays. Vision Res. 41:1261–1275.

O'Doherty JE, Lebedev MA, Ifft PJ, Zhuang KZ, Shokur S, Bleuler H, Nicolelis MA. 2011. Active tactile exploration using a brain-machine-brain interface. Nature. 479:228–231.

O'Doherty JE, Lebedev MA, Li Z, Nicolelis MA. 2012. Virtual active touch using randomly patterned intracortical microstimulation. IEEE Trans Neural Syst Rehabil Eng. 20:85–93.

Olds J, Milner P. 1954. Positive reinforcement produced by electrical stimulation of septal area and other regions of rat brain. J Comp Physiol Psychol. 47:419–427.

Pare D. 2003. Role of the basolateral amygdala in memory consolidation. Prog Neurobiol. 70:409–420.

Pare D, Collins DR, Pelletier JG. 2002. Amygdala oscillations and the consolidation of emotional memories. Trends Cogn Sci. 6:306–314.

Pavlides C, Greenstein YJ, Grudman M, Winson J. 1988. Long-term potentiation in the dentate gyrus is induced preferentially on the positive phase of theta-rhythm. Brain Res. 439:383–387.

Paxinos G, Watson C. 2009. The Rat Brain in Stereotaxic Coordinates. 6th ed. San Diego: Elsevier Academic Press.

Paz R, Bauer EP, Pare D. 2008. Theta synchronizes the activity of medial prefrontal neurons during learning. Learn Mem. 15:524–531.

Pezzone MA, Lee WS, Hoffman GE, Rabin BS. 1992. Induction of c-Fos immunoreactivity in the rat forebrain by conditioned and unconditioned aversive stimuli. Brain Res. 597:41–50.

Quinkert AW, Schiff ND, Pfaff DW. 2010. Temporal patterning of pulses during deep brain stimulation affects central nervous system arousal. Behav Brain Res. 214:377–385.

Quirk GJ. 2002. Memory for extinction of conditioned fear is long-lasting and persists following spontaneous recovery. Learn Mem. 9:402–407.

Quirk GJ, Likhtik E, Pelletier JG, Pare D. 2003. Stimulation of medial prefrontal cortex decreases the responsiveness of central amygdala output neurons. J Neurosci. 23:8800–8807.

Quiroga RQ, Reddy L, Kreiman G, Koch C, Fried I. 2005. Invariant visual representation by single neurons in the human brain. Nature. 435:1102–1107.

Racine RJ. 1972. Modification of seizure activity by electrical stimulation. II. Motor seizure. Electroencephalogr Clin Neurophysiol. 32:281–294.

Rey HG, Fried I, Quian Quiroga R. 2014. Timing of single-neuron and local field potential responses in the human medial temporal lobe. Curr Biol. 24:299–304.

Rolls ET, Treves A. 2011. The neuronal encoding of information in the brain. Prog Neurobiol. 95:448–490.

Rumelhart DE, McClelland JL. 1986. Parallel distributed processing: explorations in the microstructure of cognition. Cambridge (MA): MIT Press.

Singer W. 2009. Distributed processing and temporal codes in neuronal networks. Cogn Neurodyn. 3:189–196.

Singer W. 1999. Neuronal synchrony: a versatile code for the definition of relations? Neuron. 24:49–65, 111–125.

Singer W. 1993. Synchronization of cortical activity and its putative role in information processing and learning. Annu Rev Physiol. 55:349–374.

Smith MA, Banerjee S, Gold PW, Glowa J. 1992. Induction of c-fos mRNA in rat brain by conditioned and unconditioned stressors. Brain Res. 578:135–141.

Stuber GD, Britt JP, Bonci A. 2012. Optogenetic modulation of neural circuits that underlie reward seeking. Biol Psychiatry. 71:1061–1067.

Talwar SK, Xu S, Hawley ES, Weiss SA, Moxon KA, Chapin JK. 2002. Rat navigation guided by remote control. Nature. 417:37–38.

Toman JE. 1951. Neuropharmacologic considerations in psychic seizures. Neurology. 1:444–460.

Tort AB, Komorowski R, Eichenbaum H, Kopell N. 2010. Measuring phase-amplitude coupling between neuronal oscillations of different frequencies. J Neurophysiol. 104: 1195–1210.

Varela F, Lachaux JP, Rodriguez E, Martinerie J. 2001. The brainweb: phase synchronization and large-scale integration. Nat Rev Neurosci. 2:229–239.

Vianna DM, Borelli KG, Ferreira-Netto C, Macedo CE, Brandao ML. 2003. Fos-like immunoreactive neurons following electrical stimulation of the dorsal periaqueductal gray at freezing and escape thresholds. Brain Res Bull. 62:179–189.

Warren DJ, Fernandez E, Normann RA. 2001. High-resolution two-dimensional spatial mapping of cat striate cortex using a 100-microelectrode array. Neuroscience. 105:19–31.

Womelsdorf T, Fries P. 2006. Neuronal coherence during selective attentional processing and sensory-motor integration. J Physiol (Paris). 100:182–193.